Thermochimica Acta, 139 (1989) 181–196
Elsevier Science Publishers B.V., Amsterdam – Printed in The Netherlands

THE HEAT CAPACITY OF THE METAL HYDRIDE $TaD_{0.5}$ BETWEEN 10 and 550 K *,**

AKIRA INABA and HIDEAKI CHIHARA

Department of Chemistry and Chemical Thermodynamics Laboratory, Faculty of Science, Osaka University, Toyonaka 560 (Japan)

(Received 1 June 1988)

ABSTRACT

Heat capacity measurements have been made on $TaD_{0.5}$ between 10 and 550 K using two calorimeters of the adiabatic type in order to investigate the thermodynamic behaviour of hydrogen/deuterium in the metal. Analysis strongly suggests that a considerable amount of local order is imparted into the disordered α phase and it is then gradually thermally destroyed, suggesting that the "blocking" model is not applicable at high temperatures. In the ordered β phase, the energy required to form vacancies has been derived. A spontaneous heat evolution was observed both in the β and α phases after the system was brought through the phase transition. It is probable that the stress introduced into the metal sublattice was released either by a pre-transition effect (for the β phase) or by an annealing effect (for the α phase). The high-temperature calorimeter cell is described in detail.

INTRODUCTION

Some of the transition metals dissolve substantial quantities of interstitial solutes such as hydrogen [1]. In the lattice–gas model, a metal–hydrogen system can be regarded as a quasimonocomponent system of hydrogen atoms dissolved in the host metal lattice [2]. While quite a few calorimetric measurements for metal hydrides have been made over the years, motivated both from a theoretical as well as an applied point of view, only a limited number of the systems has been investigated, mostly by Flotow and his coworkers (see, for example, ref. 3), by precision heat capacity measurements using adiabatic calorimetry.

The purpose of the present study is to elucidate the thermodynamic behaviour of hydrogen/deuterium in tantalum, in relation to phase transi-

* Dedicated to Professor Edgar F. Westrum, Jr., in honour of his outstanding contributions to calorimetry and on the occasion of his 70th birthday.

** Contribution No. 153 from the Chemical Thermodynamics Laboratory, Faculty of Science, Osaka University.

tions of the positional order–disorder type. We undertook precise heat capacity measurements for $TaD_{0.5}$ between 10 and 550 K and compared the results with those of $TaH_{0.5}$ on which a pioneer study had taken place [4].

Neutron diffraction measurements [5] showed that in the disordered α phase, the hydrogens are randomly located at the 12 tetrahedral interstitial sites available per hydrogen in the b.c.c. tantalum. Because of the small entropy of transition (10 J K^{-1} mol^{-1}) obtained for $TaH_{0.5}$ [4], however, it is currently suspected that the presence of interstitial hydrogen blocks a certain number of neighbouring sites and prevents their occupancy [6–9]. It would, therefore, be worthwhile to establish the existence of an effect arising from local order of hydrogen in the metal, or some other effect such as an unusual isotope effect arising from anharmonic vibration of hydrogen, both of which are considered to be one of the features of such a system [10,11].

As will be described below, an excess heat capacity, distinct from the other contributions, can be interpreted as resulting from the destruction of local order in the α phase. In addition, analysis of the low-temperature part of the transition yields the energy of vacancy formation which is related to hydrogen diffusion in the metal interstices. Unexpected heat evolution encountered both in the α and the ordered β phases will also be described.

EXPERIMENTAL

Two adiabatic calorimeters were employed, the first of which covered the range from 65 to 550 K while the second extended it down to 10 K. The calorimeters and their operations are the same as those described elsewhere [12,13]. The only change made for the present experiments was that new cells were used for both calorimeters.

The high-temperature calorimeter cell is illustrated in Fig. 1. The body of the cell D is made of silver with a wall 0.3 mm thick. A vacuum-tight closure A attached to the top of the cell is made of stainless steel and is similar to the one developed by Trowbridge and Westrum, Jr. [14]. A gold gasket disk (0.5 mm thick) is forced by screw threads against a circular knife-edge in order to seal the aperture (6 mm in diameter) of the sample compartment. As a working thermometer, two pieces of platinum resistance elements H (Sensing Devices Ltd., each having 50 Ω at room temperature) are used, connected electrically in parallel and mounted onto the bottom of the cell. The calorimeter heater E (150 Ω, 0.10 mm in diameter, ceramic-insulated Nichrome wire) is wound in a bifilar manner over the cell, using boron nitride cement to bond the wires to the wall surface. The silver shells B and G are screwed at F and serve to keep the temperature uniform even during a heating period. On the side of the shell, two pockets C are provided for housing differential thermocouples. The calorimeter cell has a total mass of about 38 g with an inner volume of 8.6 cm^3.

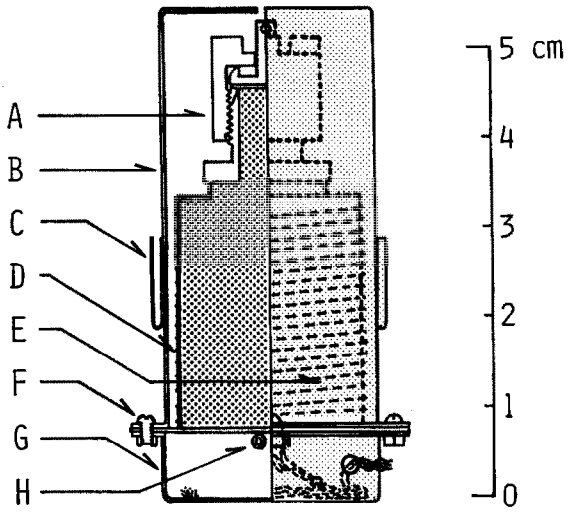

Fig. 1. High-temperature calorimeter cell: A, closure assembly; B, upper silver shell; C, pockets for thermocouples; D, body of the cell; E, calorimeter heater; F, screws; G, bottom silver shell; H, platinum resistance thermometers.

The low-temperature calorimeter cell (laboratory designation 8601) is the same as the one used before [15] except that the thermometers are replaced by a capsule-type platinum resistance thermometer (model 8164, Leeds and Northrup, labelled δ-Pt) and a germanium resistance thermometer (model GR-1000, Lake Shore). Calibrations had been made by the suppliers of these thermometers using IPTS-68 above 14 K and T-76 below 20 K, both of which are related to the temperature scales at the U.S. National Bureau of Standards.

It should be mentioned here that the platinum thermometer attached to the high-temperature calorimeter was carefully examined before use with respect to its stability [16,17] because the element is not fully strain-free, nor is it sealed. Moreover, the ratio of resistance at the steam point to that at the ice point was 1.39187 which is significantly poorer than the value specified by the IPTS (1.39250). The stability, however, proved to be acceptable: the temperatures at the triple point of water were stable within ± 4 mK for several repeated cycles in temperature between 77 and 800 K. Calibrations were then performed by intercomparison with another standard platinum thermometer [12] and also by direct comparison with several fixed points: 70, 90.188 (boiling point of oxygen), 150, 273.15 (triple point of H_2O), 302.924 (triple point of Ga), 373.15 (boiling point of H_2O), 429.779 (triple point of In) and 692.73 K (freezing point of Zn). The temperature scale was thus established, based on the IPTS-68 by introducing an additional term to the original functions of the IPTS. This thermometer has great advantages, namely that it is acceptably stable, small in size and also inexpensive.

The sample was prepared by Asano using the established method [18] of reacting deuterium gas with tantalum metal. Because of its pertinence to the discussion that will follow, it is worthwhile to describe some of the details here. Electron-beam-melted tantalum metal obtained from Tokyo Electrolysis was stated to be purer than 99.95%. The original metal from the same source had been previously examined [19] by considering its resistance ratio and its exact superconductive transition point. It was rolled into foils 0.2 mm thick, which were outgassed at 900 °C under vacuum (10^{-4} Pa) in a quartz tube and exposed to purified hydrogen gas at 600 °C. The fine powder (less than 100 mesh) obtained by crushing the hydride foils, was outgassed again at 900 °C and reduced to tantalum metal. The appropriate amount of deuterium gas was then charged to it at 600 °C using the purified gas generated by thermal decomposition of titanium deuteride. The original deuterium gas used was obtained from Showa Denko with an isotopic purity of 99.8%. The amount of gas metered in yielded a composition having a D:Ta ratio of 0.500 with an estimated uncertainty of $\pm 1\%$. An X-ray examination of this powder revealed sharp diffraction lines, suggesting that the homogenization was satisfactory.

The sample initially loaded in the high-temperature calorimeter weighed 64.854 g and contained 0.35643 mol. When the high-temperature measurements were concluded, the sample was transferred to the low-temperature calorimeter. The sample used in these measurements was 50.747 g. A small amount of helium gas was admitted to promote rapid thermal equilibrium; 20 kPa at room temperature for the high-temperature calorimeter and 0.5 kPa for the low-temperature calorimeter. The heat capacity of the empty cells was determined in advance in a separate series of measurements. The contribution of the specimen to the total heat capacity, including that of the calorimeter cell, was larger than 45% for both calorimeters over the entire temperature range.

RESULTS

The original sample, which had been prepared well before the present experiments, was cooled to 65 K in the high-temperature calorimeter and the measurements were begun. The measured heat capacities of $TaD_{0.5}$ are presented in chronological sequence in Table 1, where the temperature increment of each measurement may be deduced from the adjacent entries. They exhibited two thermal anomalies at 329.5 K and at 332 K, which fact is consistent with the previous work by DSC calorimetry [8]. But, our maximum value of the heat capacity was approximately two and a half times as large. Because the two transitions occur successively in a narrow temperature interval, the heat capacities in this region are illustrated with a semi-log plot in an expanded temperature scale (Fig. 2), where the results of $TaH_{0.5}$

TABLE 1

Molar heat capacity of $TaD_{0.5}$

T (K)	C_p (J K^{-1} mol^{-1})	T (K)	C_p (J K^{-1} mol^{-1})	T (K)	C_p (J K^{-1} mol^{-1})
High-temperature		220.52	26.64	Series 2	
calorimeter		224.58	26.93	349.25	35.73
		228.62	27.22	355.68	35.77
Series 1		232.68	27.54	363.01	35.80
66.60	13.12	236.75	27.85	370.33	35.79
68.25	13.52	240.82	28.18	377.65	35.89
69.59	13.81	244.89	28.52	384.95	35.98
71.64	14.27	248.98	28.87	392.23	36.07
73.92	14.75	252.23	29.18	399.49	36.21
76.33	15.20	255.27	29.48	406.74	36.28
78.86	15.68	258.13	29.83	413.97	36.40
81.52	16.12	261.01	30.15	421.19	36.48
84.36	16.58	263.91	30.50	428.44	36.60
87.44	17.05	266.82	30.87	435.62	36.77
90.70	17.53	269.76	31.26	442.79	36.87
94.09	17.96	272.68	31.68	449.94	37.01
97.61	18.42	275.58	32.08	457.08	37.12
101.27	18.82	278.46	32.53	464.20	37.21
105.07	19.23	281.31	33.04	471.31	37.32
109.01	19.63	284.14	33.56	478.41	37.42
113.04	20.00	286.95	34.11	485.49	37.50
117.10	20.37	289.73	34.71	492.57	37.60
121.20	20.69	292.49	35.37	499.63	37.72
125.35	21.01	295.21	36.06	506.67	37.84
129.48	21.34	297.91	36.84	513.70	37.93
133.61	21.62	300.57	37.68	520.72	38.03
137.80	21.91	303.20	38.62	527.73	38.14
141.99	22.17	305.79	39.67	534.73	38.22
146.12	22.42	308.34	40.83	541.72	38.22
150.26	22.66	310.85	42.21	548.69	38.41
154.46	22.89	313.31	43.77		
158.68	23.14	315.78	45.50	Series 3	
162.87	23.36	318.66	49.44	298.85	37.43
167.07	23.62	323.20	60.26	302.26	38.48
171.25	23.82	326.76	117.5	305.61	39.70
175.41	24.04	327.83	190.8	308.88	41.14
179.55	24.26	330.92	305.3	312.08	42.78
183.67	24.49	331.80	2134	315.18	44.86
187.79	24.70	332.00	3127	318.16	47.74
191.89	24.95	332.19	2192	321.00	52.38
195.99	25.16	334.32	93.58	323.57	62.90
200.11	25.40	338.14	36.53	325.66	92.19
204.22	25.64	340.60	35.99	327.16	145.5
208.58	25.86	346.10	35.79	328.22	204.4
212.42	26.15	351.60	35.76	329.05	250.4
216.51	26.39	357.10	35.79	329.78	263.6

TABLE 1 (continued)

T (K)	C_p (J K^{-1} mol^{-1})	T (K)	C_p (J K^{-1} mol^{-1})	T (K)	C_p (J K^{-1} mol^{-1})
330.53	239.9	11.90	0.2067	44.99	7.208
331.17	373.7	12.47	0.2236	46.40	7.631
331.68	16318	13.02	0.2550	47.82	8.086
332.03	2942	13.57	0.2762	49.23	8.506
332.17	2612	14.09	0.3082	50.66	8.940
332.27	1835	14.61	0.3390	52.09	9.339
332.79	195.4			53.53	9.756
334.80	43.81	Series 7		54.96	10.18
338.04	37.82	14.01	0.3028	56.40	10.58
341.45	37.25	14.84	0.3534	57.85	10.96
344.87	37.13	15.75	0.4339	59.29	11.34
		16.67	0.5064	60.74	11.73
Series 4		17.64	0.5891	62.19	12.12
Continuous heating		18.60	0.6815	63.65	12.46
		19.55	0.7878	65.10	12.80
Low-temperature		20.49	0.9092	66.56	13.18
calorimeter		21.48	1.042	68.02	13.51
		22.57	1.202	69.48	13.82
		23.69	1.393	70.94	14.13
Series 5		24.78	1.596	72.39	14.45
9.92	0.1272	25.91	1.818	Series 8	
10.59	0.1524	27.11	2.075		
11.23	0.1719	28.37	2.368	56.88	10.68
11.86	0.1975	29.59	2.668	58.50	11.13
12.46	0.2291	30.85	2.996	60.25	11.58
13.01	0.2477	32.31	3.384	62.09	12.06
13.50	0.2820	33.85	3.816	64.02	12.64
13.98	0.3093	35.26	4.230	65.96	12.99
		36.63	4.634	67.97	13.46
Series 6		38.01	5.051	70.11	13.94
9.64	0.1142	39.39	5.480	72.26	14.36
10.17	0.1307	40.78	5.904	74.54	14.81
10.71	0.1515	42.18	6.339	76.93	15.28
11.31	0.1737	43.58	6.778		

are also included. For $TaH_{0.5}$, an additional transition was observed at 306 K. In the transition regions, thermal relaxation time became as long as several hours or longer, whereas the temperature-equilibrium time was normally shorter than 10 min for both calorimeters.

At the end of Series 1, above 360 K, a spontaneous heat evolution was encountered. One way in which this was manifested was by way of a temperature drift ten minutes after an increment of energy had been supplied. A plot shown in Fig. 3 illustrates this. The total extra amount of heat evolved between 360 and 520 K was around 45 J mol^{-1}, estimated from

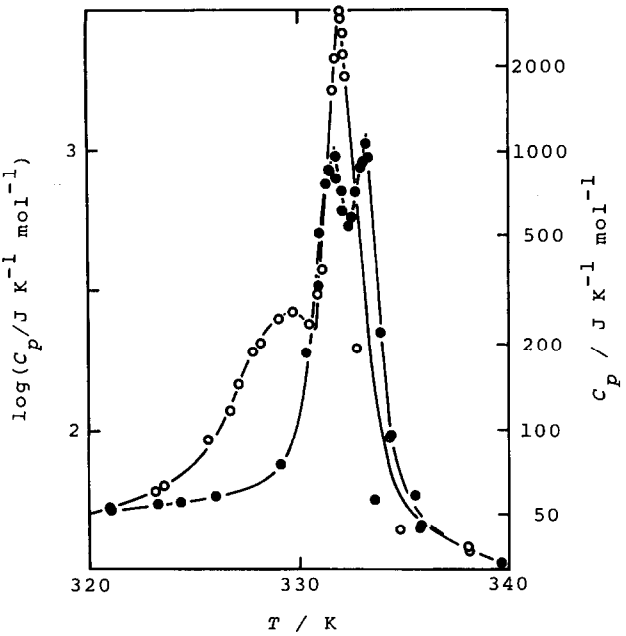

Fig. 2. Molar heat capacity of $TaH_{0.5}$ (●) and $TaD_{0.5}$ (○) in the vicinity of the phase transitions.

the drift rate, total heat capacity and the elapsed time between the two temperatures during the measurements. It should be noted that when the exothermic drift was treated in the same way as in the case of heat leakage into the sample, the calculated heat capacities, which are not included in

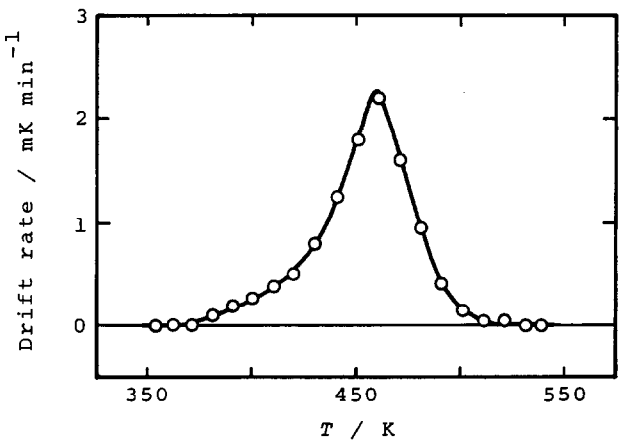

Fig. 3. Temperature drift rate as a function of temperature observed in the α phase of $TaD_{0.5}$ (Series 1).

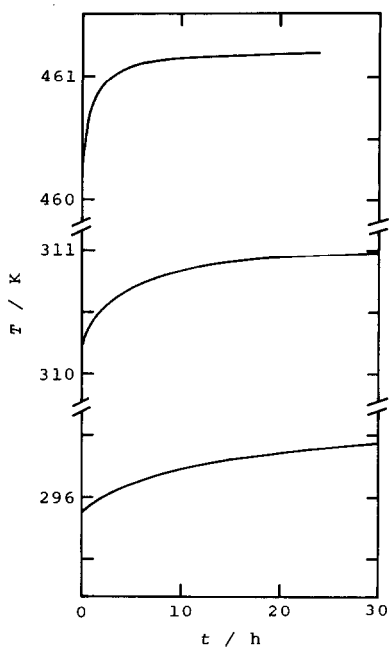

Fig. 4. Temperature drift curves showing spontaneous heat evolution in $TaD_{0.5}$.

Table 1, agreed with the heat capacities obtained in Series 2, taken after cooling to 345 K. The run, Series 2, exhibited no anomaly in relaxation. During the measurements at the beginning of Series 3, however, after the sample was cooled to the β phase, at about 200 K an appreciable exothermic drift of temperature was noticed; the drift was traced at 296 K for two whole days until no more drift was observable. The total amount of heat evolved was determined to be (45 ± 5) J mol^{-1}, which is the same magnitude

TABLE 2

Determination of the enthalpy of transition for $TaD_{0.5}$

	T_1 (K)	T_2 (K)	$H(T_2) - H(T_1)$ (J mol^{-1})	$H(338\ \text{K}) - H(301\ \text{K})$ (J mol^{-1})
Series 1 (intermittent heating)	301.884	336.232	4306.8	4412.8
Series 3 (intermittent heating)	303.938	336.425	4237.2	4414.8
Series 4 (continuous heating)	301.262	337.827	4397.0	4414.1
			Average:	4413.9

as that observed in the α phase. Since this was neither reported nor expected for $TaH_{0.5}$ [4], additional experiments were performed at the end of all the measurements with the high-temperature calorimeter to verify that the heat evolution occurs reproducibly and quantitatively. Some of the drift curves are shown in Fig. 4. While nothing certain can be deduced about why drift

TABLE 3

Thermodynamic quantities of $TaD_{0.5}$

T (K)	C_p (J K^{-1} mol^{-1})	$(H - H_0)/T$ (J K^{-1} mol^{-1})	S (J K^{-1} mol^{-1})	$-(G - H_0)/T$ (J K^{-1} mol^{-1})
10	0.128	0.03	0.04	0.01
20	0.846	0.22	0.30	0.08
30	2.775	0.71	0.96	0.25
40	5.666	1.58	2.14	0.56
50	8.740	2.70	3.73	1.03
60	11.52	3.95	5.58	1.63
70	13.91	5.20	7.54	2.34
80	15.87	6.42	9.54	3.12
90	17.43	7.56	11.49	3.93
100	18.68	8.62	13.40	4.78
110	19.72	9.58	15.23	5.65
120	20.60	10.46	16.99	6.53
130	21.38	11.27	18.67	7.40
140	22.04	12.02	20.28	8.26
150	22.64	12.71	21.82	9.11
160	23.21	13.34	23.29	9.95
170	23.76	13.94	24.72	10.78
180	24.29	14.50	26.09	11.59
190	24.83	15.03	27.42	12.39
200	25.40	15.53	28.71	13.18
210	25.97	16.02	29.96	13.94
220	26.60	16.48	31.19	14.71
230	27.33	16.94	32.38	15.44
240	28.11	17.39	33.56	16.17
250	28.97	17.83	34.73	16.90
260	30.04	18.28	35.88	17.60
270	31.29	18.74	37.04	18.30
273.15	31.75	18.88	37.40	18.52
280	32.81	19.21	38.20	18.99
290	34.78	19.71	39.38	19.67
298.15	36.99	20.15	40.38	20.23
300	37.60	20.26	40.61	20.35
350	35.74	31.33	55.52	24.19
400	36.21	31.90	60.32	28.42
450	37.01	32.42	64.61	32.19
500	37.73	32.92	68.56	35.64
550	38.43	33.39	72.18	38.79

was not observed for $TaH_{0.5}$, it is unlikely to be an isotope effect. Instead, we believe it is much more probable that the effect was overlooked for $TaH_{0.5}$, because the effect is much smaller and slower. We thus propose that the effect reflects the relaxation of stress introduced into the metal lattice through the transitions, which is consistent with the proposition that the elastic interaction between metal and hydrogen atoms plays an important role in the positional ordering of hydrogen [2]. Little can be said at this stage about the mechanism or why the heat was evolved at those temperatures. It is probable that the relaxation in the α phase was caused by the usual annealing effect whereas that in the β phase was induced by some pre-transition efffect.

A continuous heating over the transitions was made in Series 4 to obtain an accurate value for the enthalpy of transition, which agreed reasonably well with those obtained from intermittent measurements in Series 1 and 3 (Table 2).

Using the low-temperature calorimeter below 70 K, no anomaly was observed in either relaxation or heat capacity. The probable error of the heat capacities was estimated to be 0.2% over the entire temperature range except in the vicinity of the transitions and in the lowest temperature region, where it amounted to 3%. The results from the two calorimeters agree within their combined errors over the range of their overlap, around 70 K, indicating that systematic errors were probably not in excess of 0.2%.

Thermodynamic quantities were obtained from the measured heat capacity values and the enthalpy of transition. They are given at rounded temperatures in Table 3, where the small contributions below 10 K were estimated by smooth extrapolation of the heat capacity curve. It should be noted that the heat evolved from the sample is not included here.

ANALYSIS AND DISCUSSION

With regard to the analysis of the heat capacity C_p of $TaH_{0.5}$ and $TaD_{0.5}$, which we measured at virtually constant pressure, five possible contributions can be envisaged: dilation contribution $(C_p - C_v)$; lattice vibrations C_l; electronic states C_{el}; hydrogen vibrations C_h; and the transitions C_{tr} which may include other possible contributions, if any.

$$C_p = (C_p - C_v) + C_l + C_{el} + C_h + C_{tr} \tag{1}$$

$(C_p - C_v)$ is usually small for solid hydrides. It was estimated assuming the compressibility and expansivity to be the same as that for pure Ta. Its value, 0.036 J K^{-1} mol^{-1} at 400 K for example, is so relatively small that it can be neglected. The electronic contribution, $C_{el} = \gamma T$ for pure Ta was critically evaluated by Phillips [20] and a value for γ of 6.02 mJ K^{-2} mol^{-1} was chosen from the existing data which range from 5.4 to 6.3 mJ K^{-2} mol^{-1}.

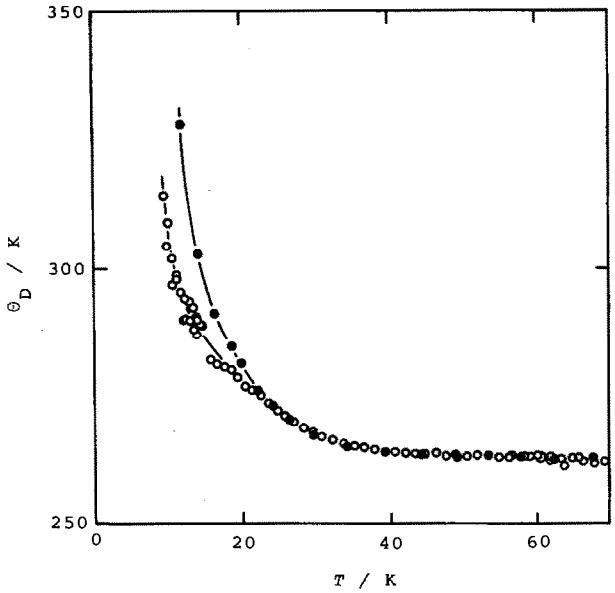

Fig. 5. Debye characteristic temperatures corresponding to the lattice heat capacities derived from $(C_p - C_{el})$ for $TaH_{0.5}$ (●) and $TaD_{0.5}$ (○).

The γ for $TaH_{0.5}$ was determined to be 2.8 mJ K^{-2} mol^{-1} by Ducastelle et al. [21]; it seems to show a significant decrease in value when tantalum is alloyed with hydrogen. However, since their value for pure Ta was evidently too small, it is more realistic to take 6.02 mJ K^{-2} mol^{-1} as the γ for $TaH_{0.5}$ and $TaD_{0.5}$.

As will be seen, the major contributions at low temperatures are made by C_l and C_{el}. Therefore, it is possible to obtain estimates of C_l from temperature variations of the equivalent Debye temperatures corresponding to the heat capacity $(C_p - C_{el})$ at low temperatures, where both C_h and C_{tr} are small. The apparent Debye temperatures thus obtained are plotted in Fig. 5. While the general shape of the $\Theta_D(T)$ curves for $TaH_{0.5}$ and $TaD_{0.5}$ is rather similar, there are significant differences below 20 K, suggesting an isotope effect in $\Theta_D(0)$ or some other anomaly. On the other hand, the flattening-off behaviour is clearly displayed above 35 K and leads to $\Theta_D(\infty) = 263$ K for both $TaH_{0.5}$ and $TaD_{0.5}$, which is higher than that for pure Ta by about 30 K, indicating that the lattice becomes harder as the metal is alloyed with hydrogen. It is reasonable to use the $\Theta_D(\infty)$ to estimate the C_{tr} at higher temperatures.

The difference in the measured heat capacities between $TaH_{0.5}$ and $TaD_{0.5}$, which is plotted in Fig. 6, should therefore come from C_h and C_{tr}. It is interesting to compare the difference with that in the C_{tr} calculated on the basis of an Einstein model using the neutron scattering results for the α phase [22,23]; 0.12 ($F = 1$) and 0.17 eV ($F = 2$) for $TaH_{0.5}$, and $0.12/\sqrt{2}$

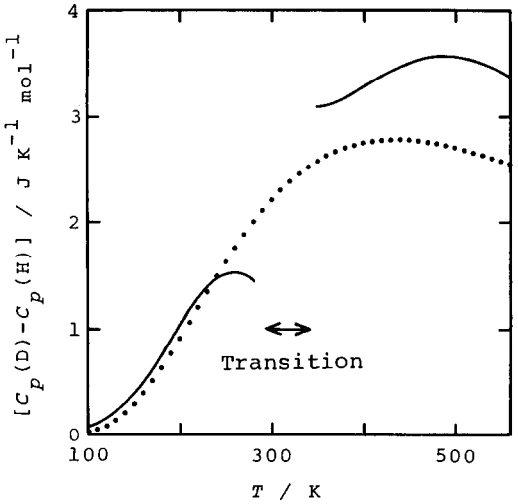

Fig. 6. Difference in measured heat capacities (———) between $TaH_{0.5}$ and $TaD_{0.5}$, compared with the calculated difference (· · · · · ·).

($F = 1$) and $0.17/\sqrt{2}$ eV ($F = 2$) for $TaD_{0.5}$, where F is the number of degrees of freedom per hydrogen/deuterium (1 eV = 96.5 kJ mol^{-1}). It is evident from Fig. 6 that while the hydrogen vibrations in the β phase can be described adequately by the harmonic vibration, the experimental results for

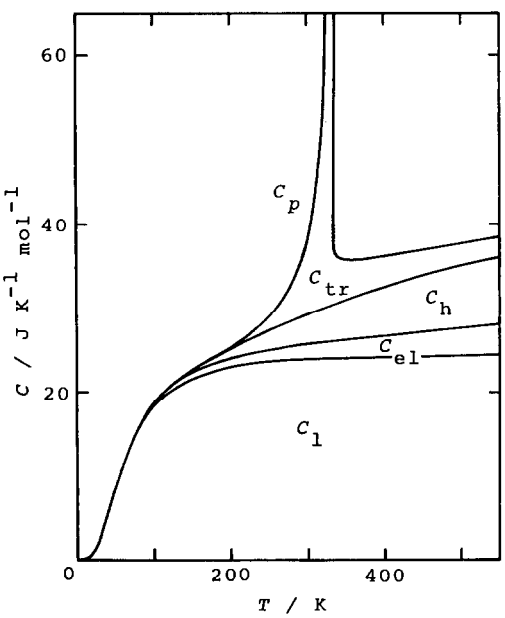

Fig. 7. Molar heat capacity of $TaD_{0.5}$ and the breakdown of the contributions from various degrees of freedom (see the text).

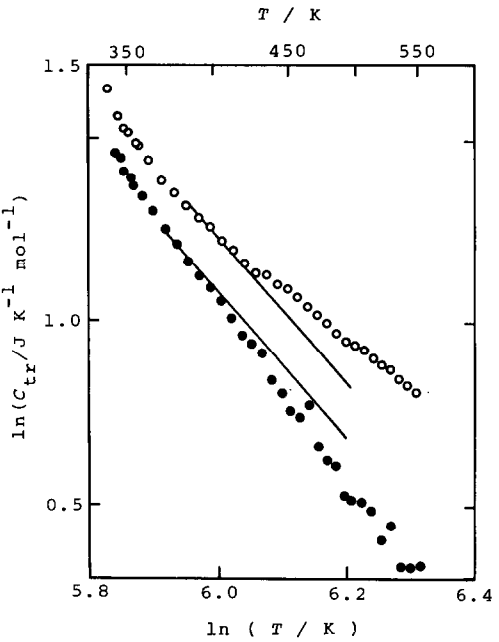

Fig. 8. Plot of $\ln C_{tr}$ against $\ln T$ for $TaH_{0.5}$ (●) and $TaD_{0.5}$ (○) showing local order in the α phase. The T^{-2} dependence is indicated for each.

the α phase deviate markedly from the calculated curve. It should be noted that the experiments of high-resolution, inelastic neutron scattering [11,24,25] found the second harmonics of those modes both in the α and β phases, whose potentials have a small anharmonicity. But, no appreciable effect could be expected on the heat capacity. This fact may allow us to argue that some other contributions such as those of local order have to be considered. The overall picture of the various contributions thus estimated for $TaD_{0.5}$ is sketched in Fig. 7.

We propose that the configurational heat capacity in the α phase is finite from the deduction described above. It is also interesting to note that C_{tr} seems to asymptotically approach zero at high temperatures. To see its convergence, a plot of $\ln C_{tr}$ against $\ln T$ was made as shown in Fig. 8. One possible interpretation of the T^{-2} dependence of the C_{tr} is that the local order would "thermally" vanish. The corresponding entropy ΔS_{tr} converges to 13.2 and 13.7 J K^{-1} mol^{-1} for $TaH_{0.5}$ and $TaD_{0.5}$, respectively, if the T^{-2} dependence is assumed above 450 K (Fig. 9). They are comparable with the entropy of 14.31 J K^{-1} mol^{-1} computed by assuming that the hydrogens are distributed randomly over all the tetrahedral interstitial sites.

The foregoing discussion depends on the choice of the value of γ. If we took γ to be 2.8 according to Ducastelle et al. [21], instead of 6.02 mJ K^{-2} mol^{-1}, the $\Theta_D(\infty)$ would become 259 K but the C_l would not be much affected by this change in $\Theta_D(\infty)$. The major change arises from C_{el}; the

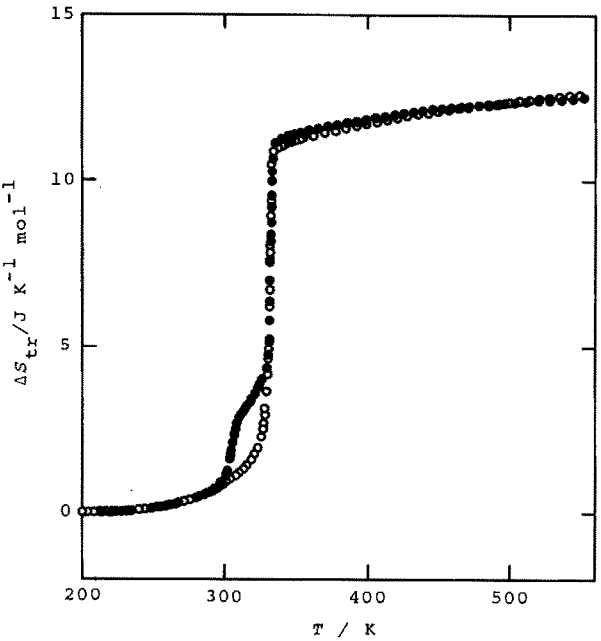

Fig. 9. Excess entropy due to the phase transitions of $TaH_{0.5}$ (●) and $TaD_{0.5}$ (○).

resulting ΔS_{tr} for $TaH_{0.5}$, for example, would already reach 14.31 J K^{-1} mol^{-1} by 560 K. This means that even greater local order would be carried over into the α phase. Such a check gives conclusive evidence of the existence of local order in the α phase. The argument given above also leads to the conclusion that the "blocking" model cannot be applied to our system at high temperatures. In fact, for some of the systems such as TiH_x [26], the sites occupied by hydrogen atoms are considered to be randomly distributed in the lattice. Although we cannot rule out the possibility that hydrogens occupy some of the octahedral sites at high temperatures, the general hypothesis based on prior information was that hydrogen atoms would exclusively enter the tetrahedral sites in the Ta/H system. It is desirable to obtain a more accurate value of γ.

In analogy with the case of melting [27], it is possible to estimate the energy required to form a kind of vacancy from the excess heat capacity ΔC_p, that is, the low-temperature tail of the transition, because transition can be described by positional disorder. Reference 27 showed that, if $\ln(T^2\Delta C_p)$ is plotted against $1/T$ (Fig. 10), one should get a straight line whose slope is $-\epsilon/k$, where ϵ is the energy required to form vacancies at the tetrahedral interstices of the ordered matrix. The estimate of ΔC_p was done by subtracting the $(C_l + C_{el} + C_h)$ from the measured C_p. While the rapid increase in the value of $\ln(T^2\Delta C_p)$ at the high temperature end is undoubtedly due to the appearance of the strong co-operative effect of the

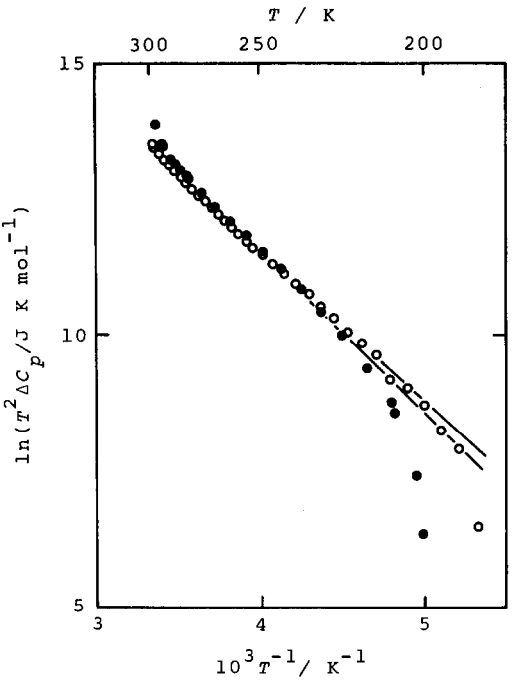

Fig. 10. Plot of $\ln(T^2\Delta C_p)$ against $1/T$ for $TaH_{0.5}$ (●) and $TaD_{0.5}$ (○).

transition, the slopes of the straight line portion give 25 and 23 kJ mol^{-1} for $TaH_{0.5}$ and $TaD_{0.5}$, respectively. In the case of simple molecular solids, the energy normally amounts to one-half (for hydrogen halides [28]) to two-thirds (for rare gases [27]) of the enthalpy of sublimation at 0 K, which reflects the relaxation of the surrounding molecules into the vacancy. The energies deduced in our systems are not inconsistent with the results of the second harmonics of hydrogen vibrations. On the other hand, it is interesting to note that the activation energies of hydrogen diffusion obtained from the other experiments are very small and of the same size as the fundamentals of the hydrogen vibrations: NMR (0.18 eV [29]); neutron experiment (0.14 eV [30]); Gorsky effect (0.14 eV [30]); and Mössbauer effect (0.14 eV [31]). They clearly demonstrate the quantum effect of diffusion, which is one of the features of these systems.

ACKNOWLEDGEMENT

The authors should like to thank Dr. H. Asano for preparing the specimen and for helpful discussion. This work was supported by Grant-in-aid for Scientific Research granted by the Ministry of Education, Science and Culture of Japan.

REFERENCES

1 For review see: T. Springer, in G. Alefeld and J. Völkl (Eds.), Hydrogen in Metals 1, Topics in Applied Physics Vol. 28, Springer, Berlin, Heidelberg and New York, 1978.
2 G. Alefeld, Phys. Status Solidi, 32 (1969) 67.
3 F.L. Oetting, A.E. Hodges III, J.M. Haschke and H.E. Flotow, J. Chem. Thermodyn., 16 (1984) 1089.
4 W.G. Saba, W.E. Wallace, H. Sandmo and R.S. Craig, J. Chem. Phys., 35 (1961) 2148.
5 W.E. Wallace, J. Chem. Phys., 35 (1961) 2156.
6 W.A. Oates, J.A. Lambert and P.T. Gallagher, Trans. Metall. Soc. AIME, 245 (1969) 47.
7 H. Buck and G. Alefeld, Phys. Status Solidi B, 47 (1971) 193.
8 H. Asano, Y. Ishino, R. Yamada and M. Hirabayashi, J. Solid State Chem., 15 (1975) 45.
9 G. Boureau, J. Phys. Chem. Solids, 42 (1981) 743.
10 H. Sugimoto and Y. Fukai, J. Phys. Soc. Jpn., 50 (1981) 3709.
11 R. Hempelmann, D. Richter and A. Kollman, Z. Phys. B, 44 (1981) 159.
12 A. Inaba, J. Chem. Thermodyn., 15 (1983) 1137.
13 K. Saito, T. Atake and H. Chihara, J. Chem. Thermodyn., 19 (1987) 633.
14 J.C. Trowbridge and E.F. Westrum, Jr., J. Phys. Chem., 67 (1963) 2381.
15 K. Saito, T. Atake and H. Chihara, J. Chem. Thermodyn., 19 (1987) 633.
16 A. Inaba, Netsu Sokutei, 10 (1983) 97, in Japanese.
17 A. Inaba, H. Fujii and M. Sakiyama, Netsu Sokutei, 11 (1984) 3, in Japanese.
18 H. Asano and M. Hirabayashi, Phys. Status Solidi A, 15 (1973) 267.
19 A. Inaba, Jpn. J. Appl. Phys., 19 (1980) 1553.
20 N.E. Phillips, Crit. Rev. Solid State Sci., (1971) 467.
21 F. Ducastelle, R. Caudron and P. Costa, J. Phys. Chem. Solids, 31 (1970) 1247.
22 J.J. Rush, R.C. Livingston, L.A. de Graaf, H.E. Flotow and J.M. Rowe, J. Chem. Phys., 59 (1973) 6570.
23 A. Magerl, N. Stump, W.D. Teuchert, V. Wagner and G. Alefeld, J. Phys. C, 10 (1977) 2783.
24 S. Ikeda, N. Watanabe and K. Kai, Physica B, 120 (1983) 131.
25 R. Hempelmann, Z. Phys. Chem. N.F., 154 (1987) 221.
26 B. Stalinski, C.K. Coogan and H.S. Gutowsky, J. Chem. Phys., 34 (1961) 1191.
27 R.H. Beaumont, H. Chihara and J.A. Morrison, Proc. Phys. Soc. London, 78 (1961) 1462.
28 A. Inaba and H. Chihara, J. Chem. Thermodyn., 10 (1978) 65.
29 P.E. Mauger, W.D. Williams and R.M. Cotts, J. Phys. Chem. Solids, 42 (1981) 821.
30 G. Schaumann, J. Völkl and G. Alefeld, Phys. Status Solidi, 42 (1970) 401.
31 A. Heidemann, G. Kaindl, D. Salomon, H. Wipf and G. Wortmann, Phys. Rev. Lett., 36 (1976) 213.